Tellus (2007), 59B, 191–198
Printed in Singapore. All rights reserved

TELLUS

Climate change feedbacks on future oceanic acidification

By BEN I. MCNEIL[1]* and RICHARD J. MATEAR[2], [1]*Climate & Environmental Dynamics Laboratory, School of Mathematics and Statistics, University of New South Wales, Sydney, NSW, Australia;* [2]*CSIRO Marine Research and Antarctic, Climate and Ecosystem CRC, Hobart, Australia*

(Manuscript received 9 February 2006; in final form 9 November 2006)

ABSTRACT

Oceanic anthropogenic CO_2 uptake will decrease both the pH and the aragonite saturation state (Ω_{arag}) of seawater leading to an oceanic acidification. However, the factors controlling future changes in pH and Ω_{arag} are independent and will respond differently to oceanic climate change feedbacks such as ocean warming, circulation and biological changes. We examine the sensitivity of these two CO_2-related parameters to climate change feedbacks within a coupled atmosphere-ocean model. The ocean warming feedback was found to dominate the climate change responses in the surface ocean. Although surface pH is projected to decrease relatively uniformly by about 0.3 by the year 2100, we find pH to be insensitive to climate change feedbacks, whereas Ω_{arag} is buffered by ~15%. Ocean carbonate chemistry creates a situation whereby the direct pH changes due to ocean warming are almost cancelled by the pH changes associated with dissolved inorganic carbon concentrations changes via a reduction in CO_2 solubility from ocean warming. We show that the small climate change feedback on future surface ocean pH is independent to the amount of ocean warming. Our analysis therefore implies that future projections of surface ocean acidification only need to consider future atmospheric CO_2 levels, not climate change induced modifications in the ocean.

1. Introduction and background

Rising atmospheric CO_2 concentrations via fossil fuel emissions will lead to an increase in oceanic CO_2 as the ocean attempts to re-equilibrate with the perturbed atmosphere (McNeil et al., 2003). Increased CO_2 in the upper ocean will alter the chemical speciation of the oceanic carbon system. As CO_2 enters the ocean it undergoes the following reactions:

$$CO_2 + H_2O \Leftrightarrow H_2CO_3 \Leftrightarrow HCO_3^- + H^+ \Leftrightarrow CO_3^{2-} + 2H^+ \quad (1)$$

Two important parameters of the oceanic carbon system are the pH and the $CaCO_3$ saturation state of seawater (Ω). The $CaCO_3$ saturation state of seawater (Ω) is defined by: $\Omega = \frac{[Ca^{2+}][CO_3^{2-}]}{\lambda}$, where λ is the solubility coefficient of different forms of $CaCO_3$ (e.g. calcite and aragonite). The pH of seawater is defined by the total amount of H^+ ions available (Dickson, 1993).

Increasing CO_2 concentrations in the surface ocean via anthropogenic CO_2 uptake will have two effects. First, it decreases the surface ocean carbonate ion concentration (CO_3^{2-}) and decreases the calcium carbonate saturation state (Ω). Using an ocean-only model forced with atmospheric CO_2 projections (IS92a), (Kleypas et al., 1999) predicts a 40% reduction in Ω_{arag} by 2100. Laboratory experiments have shown some species of corals and calcifying phytoplankton (Gattuso et al., 1998; Langdon et al., 2000) are highly sensitive to changes in Ω_{arag} which have led to the hypothesis of large decreases in future calcification rates under elevated atmospheric CO_2 (Kleypas et al., 1999). Secondly, when CO_2 dissolves in water it forms a weak acid (H_2CO_3), (eq. 1) dissociates to bicarbonate generating hydrogen ions (H^+), which makes the ocean more acidic (pH decreases). Using an ocean-only model forced with atmospheric CO_2 projections (IS92a), (Caldeira and Wickett, 2003) predicts a pH drop of 0.4 units by the year 2100 and a further decline of 0.7 by the year 2300. They find the oceanic absorption of anthropogenic CO_2 over the next several centuries may result in a pH decrease greater than inferred from the geological record over the past 300 million years, with the possible exception of those resulting from rare, extreme events such as bolide impacts.

Future acidification (lowering of pH) may adversely impact marine biota (Raven, 2005), but our understanding of the biological response is limited. It is recognised however that a decrease in pH will alter the acid–base balance within the cells of marine organisms. Marine organisms regulate intercellular pH by the metabolic interconversion of acids and bases, the passive chemical buffering of intra and extracellular fluids, and the active ion transport (e.g. proton transport by extracellular

*Corresponding author.
e-mail: b.mcneil@unsw.edu.au
DOI: 10.1111/j.1600-0889.2006.00241.x

respiratory proteins such as hemoglobin) (Walsh and Milligan, 1989). Acid–base imbalances in marine organisms can lead to the dissolution of exoskeletal components such as calcareous shells, metabolic suppression, reduced protein synthesis and reduced activity (Seibel and Walsh, 2001; Seibel and Walsh, 2003). Experiments to determine the likely response of marine organisms to pH changes have explored large changes in pH (>1) under laboratory conditions (Kikkawa et al., 2003; Pedersen and Hansen, 2003a, b; Portner et al., 2004; Barry et al., 2004; Engel et al., 2005). Little is known on what the gradual long-term effects of pH lowering will be on marine organisms. As both Ω_{arag} and pH changes have the potential to directly impact marine biota it is important to understand the magnitude of these changes under elevated CO_2 levels and global warming.

Projections of future decreases in both pH and Ω have been obtained from ocean-only models (Caldeira and Wickett, 2003; Kleypas et al., 1999), however these modelling studies have not considered the effect of climate change feedbacks on the carbon chemistry of the ocean. Recently however, a study explored the significance that climate change plays on the extent of ocean acidification (Orr et al., 2005). Using three separate climate models they found climate change to insignificantly impact the projected future decreases of pH, but significantly impact Ω. However due to brevity, the study could not explore either the reason or importance of independent feedbacks on oceanic acidification. In this study we compliment the previous study by using coupled atmosphere-ocean model to examine and explore the importance of climate change feedbacks on surface ocean pH and Ω. We use the model simulations to explore the relationship between climate change and these two carbon parameters on both a global and regional scale so as to better project future changes in these parameters and enable an improved assessment of the potential impacts they may have on marine organisms.

2. Climate model

To explore climate change feedbacks on carbon chemistry we use a coupled atmosphere-ice-ocean carbon cycle model developed by the Commonwealth Scientific Industrial Research Organisation (CSIRO) (Hirst et al., 1996). Differing climate models maintain differing sensitivities to anthropogenic climate forcing. The sensitivity is defined as the global annual temperature change associated with a doubling of atmospheric CO_2. The sensitivity of the CSIRO Mark II climate model is 4.3 °C (Watterson et al., 1997), and is at the higher range of global model sensitivities (Houghton et al., 2001). The CSIRO climate model includes oceanic, sea–ice and biospheric submodels with oceanic eddy parameterization. The oceanic submodel includes a prognostic ocean carbon cycle model that simulates phosphate, DIC and alkalinity in the ocean. The rain ratio of biological carbon export (PIC/POC) was constant at 0.08 while traditional Redfield ratios were used for organic matter export stoichiometry. CO_2 dissociation constants of (Dickson and Millero, 1987) were used to determine pCO_2, pH and Ω within the model. Air–sea fluxes of CO_2 were simulated using the (Wanninkhof, 1992) gas exchange formulation. Climate change feedbacks were quantified using two separate climate model experiments. The 'control' experiment that did not include the warming effects of elevated greenhouse gases in the atmosphere (no additional radiative forcing) and the 'climate change' experiment that explicitly included the radiative forcing of greenhouse gases in the atmosphere (Matear and Hirst, 1999). For the climate change experiment, atmospheric CO_2 levels increased according to observations between 1880 and 1995 then followed IS92a projections until the year 2100 (Houghton et al., 2001). The climate change feedback on carbon chemistry was taken to be the difference between the 'climate change' experiment and the 'control' experiment and includes effects such as changes to the thermohaline circulation, temperature, salinity and the biological carbon flux.

3. Comparison with oceanic measurements

To assess the spatial distribution of the simulated surface pH and Ω we compare our model results to observations. (Key et al., 2004) have compiled a global synthesis of oceanic carbon measurements made during the World Ocean Circulation Experiment between the year 1991 and 1998 (http://cdiac.esd.ornl.gov/oceans/glodap/Glodap˙home.htm). From this dataset we calculate the zonally averaged surface pH and Ω_{arag} and then compare it to our model output. For the year 1995, surface ocean pH variability in our model simulation is relatively small (8–8.2) and consistent with the observations (Fig. 1a). In contrast, the observations show large spatial variations in Ω_{arag} for the year 1995 (1.5–4.4), which is also consistent with our model simulation (Fig. 1b). For surface pH, the model shows a systematic decrease has already occurred ($\sim$0.1) between the year 1880 and 1995 that is beyond the range of observed spatial variability (i.e. 25th/75th percentile). Spatial variability is much greater for surface Ω_{arag} and the decrease between 1880 and 1995 is still within the spatial variability of Ω_{arag}. Some regions such as the North Atlantic (>50°N) actually show no measurable change based on the observations (Fig. 1b). In general our model simulations match the observations and give us confidence to explore the future climate change feedbacks within the CSIRO climate model.

4. Results and discussion

Changes in surface pH and in Ω_{arag} reflect changes in the speciation of carbon within the ocean and are a function of temperature, salinity, alkalinity and DIC concentrations. With climate change, the model projects average sea surface temperature (SST) to warm from 18 °C to about 21.5°C by the year 2100 (Fig. 2b) while the globally averaged sea surface salinity (SSS) freshens from 34.71 to 34.53 (Fig. 2c). Salinity normalized Alkalinity

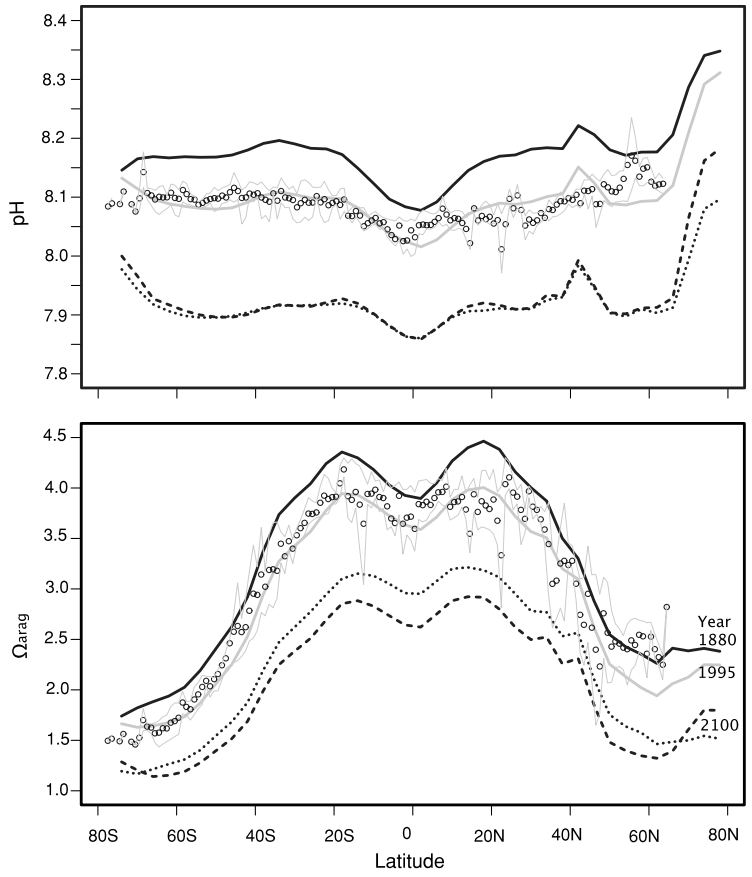

Fig. 1. Zonally averaged change in surface ocean CO_2 chemistry from 1880 to 2100. (A) pH and (B) Ω_{arag}. Solid black line is for the year 1880, dashed line is for the year 2100 under the control experiment and the dotted line is for the year 2100 under the climate change experiment. The circles show the average calculated values using the global carbon observations (1991–1998) from (Key et al., 2004) using dissociation constants from (Dickson and Millero, 1987). The light-grey lines around the observations are the 25th and 75th quantiles to illustrate the range of natural variability. The solid drak-grey line is the model prediction for the year 1995 and serve as a direct comparison to the observations.

remained nearly constant at an average global concentration of 2270 μmol/kg.

By 2100, the change in surface ocean DIC concentration is 18% less in the climate change simulation than in the control simulation (decline from 135 to 110 μmol/kg; see Fig. 2d). This lowered DIC concentration with climate change is due to the reduction in CO_2 solubility in surface waters due to ocean warming. If we correct the DIC concentration of the climate change simulation for the solubility reduction due to surface warming, the resulting DIC concentration is virtually identical to the DIC concentration of the control simulation (Fig. 2d). The similarity in DIC concentrations illustrates the ocean warming feedback is the dominant process regulating the inorganic carbon system in the surface ocean.

Despite the dominance of temperature in inducing climate change feedbacks, our simulations show different climate change responses for pH and Ω_{arag}. We find pH to be insensitive to climate change with virtually no difference between the transient and control experiment (Fig. 2e). For both experiments, the globally averaged surface pH is projected to decrease from 8.17 in the year 1880 to about 7.91 by 2100. Ω_{arag} however, is affected by climate change feedbacks (Fig. 2f). Globally averaged Ω_{arag} is found to decrease from 3.5 to 2.2 between 1880 and 2100 without climate change, but the decrease slows to about 2.5 when including the affects of climate change. For Ω_{arag}, this means that climate change buffers it decrease by ∼15%, although the magnitude is regionally dependent (Fig. 1b). In the Southern Ocean for example, this buffering is only of the order of ∼5%. Using three climate models Orr et al. (2005) typically found climate change feedbacks to increase $[CO_3^{2-}]$ by about 10% on the global scale. The CSIRO model suggests a higher climate change feedback most likely due to a higher climate sensitivity than the other models used by Orr et al. It will be important to explore the magnitude of climate change buffering on Ω_{arag} for a range of different models since it has been shown to be an important controlling factor for coral reef calcification along with ocean warming (McNeil et al., 2004).

4.1. Climate change feedbacks and their importance

Climate change has the potential to alter the surface ocean carbon characteristics. The three main processes which will influence the carbon system and are interrelated are : circulation driven changes, biological induced changes (both organic and inorganic) and ocean warming (direct warming effect and CO_2 solubility driven effect). Matear and Hirst (1999) showed that surface water freshening induces stratification of the oceanic overturning circulation. This climate change induced slowdown

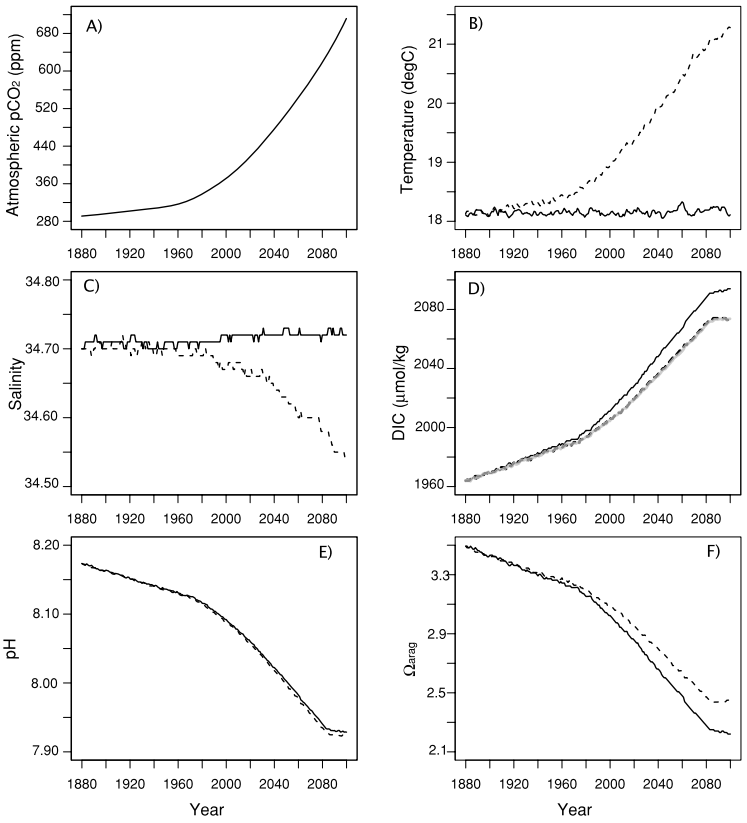

Fig. 2. (A) IS92a atmospheric CO_2 projections used by our model; (B) globally average sea surface temperature from the control experiment (solid line) and climate change experiment (dashed line); (C) globally average sea surface salinity; (D) globally averaged Dissolved Inorganic Carbon (DIC) concentration (μmol/kg) with the additional grey line illustrating the solubility-effect; (E) globally averaged pH and (F) globally averaged Ω_{arag}.

in overturning also reduces oceanic CO_2 uptake considerably. A stratified ocean also reduces the vertical re-supply of nutrients to the mixed layer for biological production and they correspondingly also show a large decrease in organic carbon export with climate change. These changes in circulation/biology impact the uptake and sequestration of CO_2 in the ocean interior and would indeed invoke small changes within the interior of the ocean. However, it is important to note that this study focuses on the surface ocean where the DIC *transient change* is dominated by air–sea equilibration with the atmosphere. The circulation and/or biologically induced DIC changes are therefore less important on *surface* DIC concentration than the effect of ocean warming as demonstrated by Fig. 2d.

To quantify what is driving the climate change feedbacks for pH and Ω_{arag}, we compare the change in pH and in Ω_{arag} between the control experiment and climate change experiment for each individual water property change (i.e. $\Delta\text{pH} = \frac{\partial \text{pH}}{\partial \text{SST}}\Delta\text{SST} + \frac{\partial \text{pH}}{\partial \text{Sal}}\Delta\text{Sal} + \frac{\partial \text{pH}}{\partial \text{ALK}}\Delta\text{ALK} + \frac{\partial \text{pH}}{\partial \text{DIC}}\Delta\text{DIC}$). Future variations in salinity and alkalinity have little effect on pH and Ω_{arag}, while the effects of DIC and SST dominate (Fig. 3).

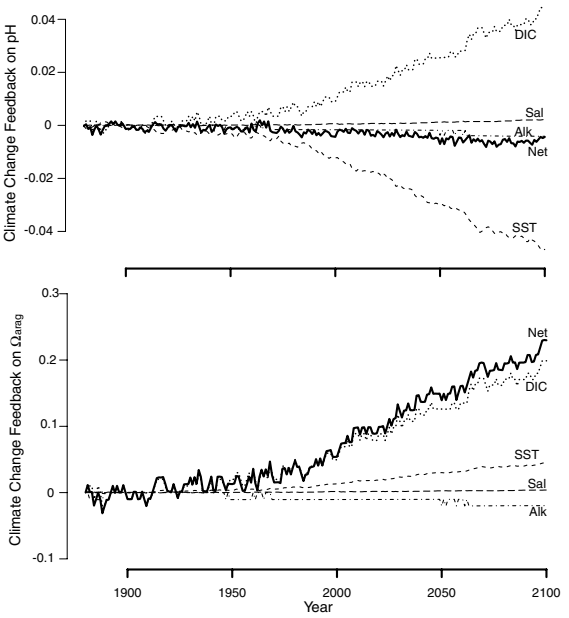

Fig. 3. Net climate change effects on pH and Ω_{arag} between 1880 and 2100 due to various parameters. Solid line represents the net climate change feedback while the dashed lines indicate changes due to DIC (exclusively indirect solubility effects from warming), SST (direct warming effect), alkalinity and salinity.

4.2. *Why is the climate change feedback on pH insignificant?*

Our simulations show that the net climate change feedback on pH (defined here as ΔpH) is close to 0 (Figs. 2e and 3a). To explore

why this is the case it is best to mathematically conceptualise the changes. Given that changes in SST and DIC are the dominant effects (Fig. 3a), the climate change feedback on pH can be written as:

$$\Delta\mathrm{pH} = \frac{\partial \mathrm{pH}}{\partial \mathrm{SST}}\Delta\mathrm{SST} + \frac{\partial \mathrm{pH}}{\partial \mathrm{DIC}}\Delta\mathrm{DIC} \quad (2)$$

Using the assumption that surface ocean DIC is in equilibrium with the atmosphere and that DIC is only affected by SST as shown by Fig. 2d, we can re-write eq. (2) as:

$$\begin{aligned}\Delta\mathrm{pH} &= \frac{\partial \mathrm{pH}}{\partial \mathrm{SST}}\Delta\mathrm{SST} + \frac{\partial \mathrm{pH}}{\partial \mathrm{DIC}}\frac{\partial \mathrm{DIC}}{\partial \mathrm{SST}}\Delta\mathrm{SST} \\ &= \underbrace{\frac{\partial \mathrm{pH}}{\partial \mathrm{SST}}\Delta\mathrm{SST}}_{\substack{\text{Direct SST}\\ \text{Feedback}}} + \underbrace{\frac{\partial \mathrm{pH}}{\partial \mathrm{DIC}}\alpha\Delta\mathrm{SST}}_{\substack{\text{In-direct SST}\\ \text{Feedback}}} \quad ; \\ &\qquad \text{where } \alpha \text{ is the solubility term.} \quad (3)\end{aligned}$$

From eq. (3) we can see that the in-direct SST feedback is that associated with DIC changes due to temperature-driven solubility changes. For pH, the direct SST feedback (left-hand side of eq. 3) is negative while the in-direct SST feedback (i.e. solubility changes in DIC; right-hand side of eq. 3) is positive (Fig. 3a). This creates a situation where the temperature related feedbacks close to cancel, resulting in the net pH feedback being insignificant (Fig. 3a).

Figure 2 showed that the difference in the globally-averaged surface DIC concentration of the control and climate change experiment primarily reflected changes in DIC due to the temperature-driven CO_2 solubility differences between these two runs. The solubility driven reductions in the surface DIC concentration due to warming increase pH by the magnitude that is almost equal to pH decline due to direct ocean warming, which cause the two affects to almost cancel each other. Figure 4a better illustrates the influence of DIC and SST on pH in relation to the evolution of both the control and climate change experiments from the model. In Fig. 4, the lines of constant pH are almost parallel to slope of the $(\frac{\partial \mathrm{DIC}}{\partial \mathrm{SST}})|_{\mathrm{ALK,Sal},\, pCO_2=\mathrm{constant}}$ due to solubility changes in CO_2. This results in the surface pH almost being independent of the magnitude of the ocean warming. Therefore, the almost complete cancellation of the change in pH due to direct and in-direct temperature effects will arise irrespective of the type or sensitivity of the climate model used.

4.3. *Independent response of pH and aragonite saturation state*

The difference between the pH and the Ω_{arag} response to climate change feedbacks reflects how increasing temperature impacts these two variables. For Ω_{arag}, the direct SST feedback on Ω_{arag} is weak (Fig. 3b), whereas the solubility induced DIC feedback is significantly negative and results in a net buffering (increase)

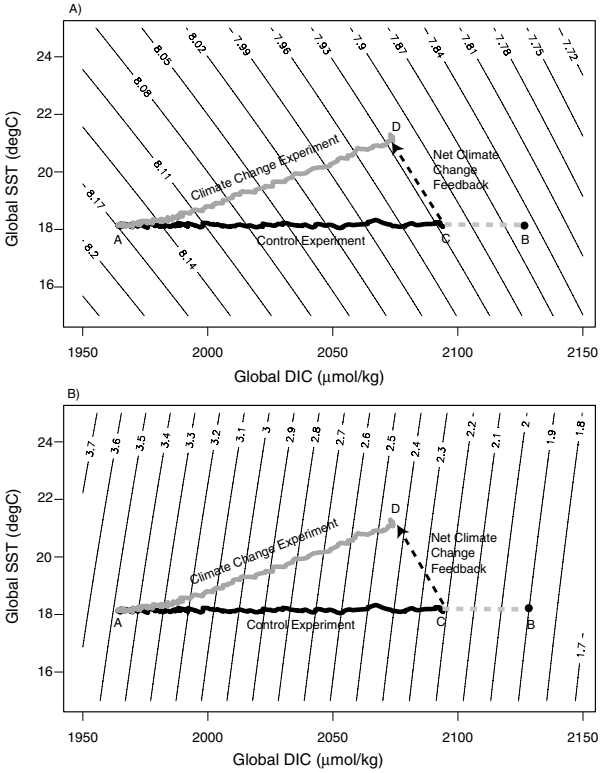

Fig. 4. (A) Evolution of mean surface pH in relation to DIC and sea surface temperature for both the control experiment (solid black line) and climate change experiment (solid grey line). The *net* climate change feedback is shown as the dashed black vector between the control and climate change experiments. Point A is the initial state in the year 1880 before industrialization. Point B is the pH state (∼7.82) in the year 2100 if the ocean absorbed atmospheric CO_2 under equilibrium proportions. Point C is the pH state (∼7.93) in the year 2100 for the control experiment and is equivalent to an oceanic steady state solution. Point D is the pH state (∼7.93) for the year 2100 under climate change, and includes feedbacks such as circulation, biological production and temperature. (B) Evolution of mean surface Ω_{arag} with same descriptions as in (A).

for Ω_{arag} of ∼0.25 by the year 2100. This is quite different to the pH response as highlighted earlier.

Figure 4 better illustrates the different influences of DIC and SST on pH and Ω_{arag} in relation to the evolution of both the control and climate change simulations. In Fig. 4, the evolution of pH and Ω_{arag} from 1880 to 2100 for the control experiment is illustrated by line A–C, while line A–D is the evolution of the climate change experiment. In the control experiment, there is no change in SST while oceanic uptake of anthropogenic CO_2 increases DIC concentration (by ∼135 μmol/kg), which consequently lowers both pH and Ω_{arag} considerably. Under climate change, SST increases while DIC concentration increases to a lesser extent than for the control due to lower CO_2 solubility (by ∼110 μmol/kg). The difference between points C and D shows

the net effect of climate change on pH and Ω_{arag}. For pH, point C and D (net climate change feedback) lie almost exactly on contours of constant pH, therefore implying that climate change has no net affect on the projected pH values as discussed earlier. For Ω_{arag}, the magnitude and direction of the SST feedback contrasts with pH, as the 3°C warming actually increase Ω_{arag} slightly. Coupling this with the reduced DIC accumulation due to solubility reductions results in a substantial buffering of Ω_{arag} with climate change.

4.4. Simulated regional changes

On a global basis, pH and Ω_{arag} respond with differing direction and magnitudes to climate change feedbacks. However, it is important to investigate this on a regional scale to identify if there are any regional deviations from this general trend. Figure 5(a,b) shows the zonal evolution of pH and Ω_{arag} in the surface ocean up to the year 2100. pH declines zonally in a relatively uniform way (0.3 units by 2100) with the exception in the Arctic Ocean where the decline is greater (∼0.4). The zonal Ω_{arag} changes are much less uniform than the pH changes with the largest decline in the mid-latitudes (40°S to 40°N). The main reason why Ω_{arag} shows the largest decrease in the mid-latitudes relates to the homogenous buffer factor (or Revelle Factor) (Sundquist et al., 1979). The Revelle factor is controlled predominantly by the $[CO_3^{2-}]$ (carbonate ion) and is a measure of the ability for the ocean to absorb CO_2 (Broecker and Peng, 1982). The mid-latitudes maintain lower Revelle factors (which means higher carbonate ion) than the rest of the ocean and therefore have a greater capacity to absorb anthropogenic CO_2 (McNeil et al., 2003). Therefore the Ω_{arag} declines are most pronounced in the mid-latitudes where the largest accumulation of anthropogenic CO_2 accumulates.

Figure 5 (c and d) show the zonal evolution of pH and Ω_{arag} associated with the net climate change feedback. For pH, there is very little variation in the magnitude and structure of the meridional change in pH due to climate change. In the Arctic Ocean (>60°N) however, there is a positive feedback and a faint positive feedback in the high Southern Ocean (>65°S) beyond the year 2070. Currently in these regions CO_2 is under-saturated with respect to the atmosphere due to both deep water ventilation along with sea-ice limitation on gas exchange (Anderson and Jones, 1991; McNeil et al., 2001). With climate change however, a reduction in sea-ice extent in these high latitudes will allow a greater degree of CO_2 saturation (and greater anthropogenic CO_2 accumulation) which is independent of ocean warming and reduces pH beyond that of other parts of the ocean. The climate change signal for Ω_{arag} shows large meridional differences both in magnitude and structure. The largest increases (or buffering) due to climate change are found in the mid-latitudes (∼0.25). Since the direct effects of ocean warming on Ω_{arag} is weak (see Fig. 3b), the zonal changes in Ω_{arag} due to climate change mostly reflect changes in anthropogenic CO_2 accumulation, caused by the reduction in CO_2 solubility associated with ocean warming. However, for the high latitudes (poleward of 60°N and 65°S), climate change actually enhances the reduction in Ω_{arag} (positive feedback) by up to −0.1. The positive feedback reflects the increase in surface anthropogenic CO_2 due to a decline in sea-ice extent allowing a higher degree of CO_2 equilibration with the atmosphere.

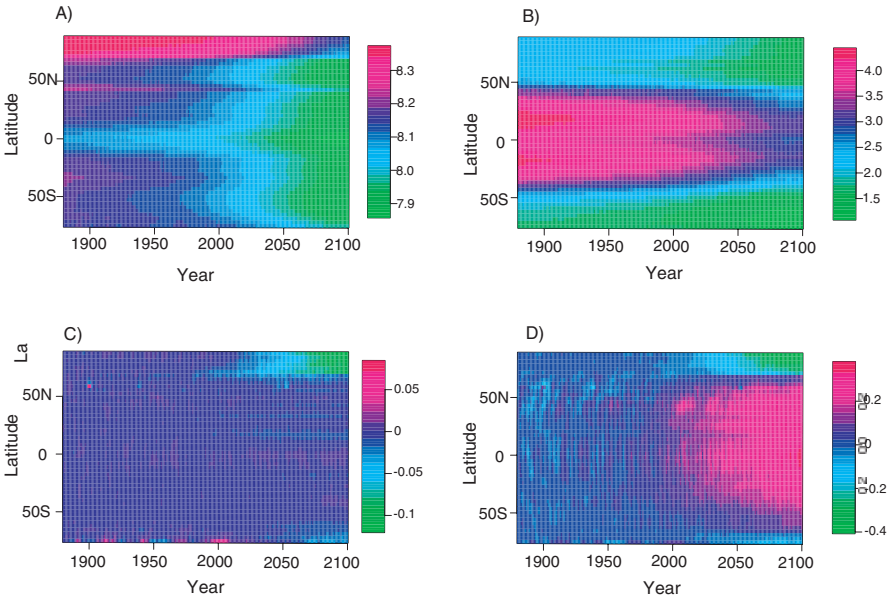

Fig. 5. A) Zonal evolution of surface ocean pH from the climate change experiment; B) surface ocean Ω_{arag}. C) Simulated zonal evolution of ΔpH due to net climate change feedbacks (C) and $\Delta\Omega_{arag}$ due to net climate change feedbacks (D).

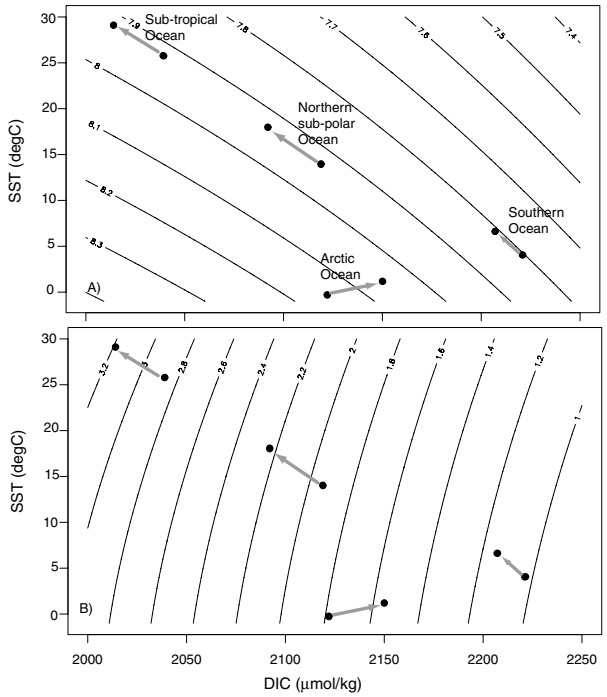

Fig. 6. (A) The net regional climate change feedback in the year 2100 for surface pH contoured in relation to DIC and sea surface temperature. The *net* climate change feedback for each region in the year 2100 is shown as the grey vector. The Southern Ocean is taken to be waters south of 40°S. The subtropical ocean are defined as waters between 30°S and 30°N. The northern subpolar ocean is between 30°N and 60°N. The Arctic Ocean are waters north of 60°S. (B) The net regional climate change feedback in the year 2100 for surface Ω_{arag} with same descriptions as in (A).

To better illustrate the regional differences due to climate change, we have split the surface ocean into four very broad regimes: subtropical (30°N–30°S), northern subpolar (30°N–60°N), Southern Ocean (>40°S) and the Arctic Ocean (>60°N). Figure 6 shows the net climate change feedback for each of these regions. Although the magnitude of the vectors change between the Southern, subtopical and northern subpolar oceans, climate change has the effect of decreasing DIC and increasing SST which coincides with parallel lines of constant pH. For Ω_{arag} however, the climate change response for these three regions is nearly perpendicular to the lines of constant Ω_{arag}, which causes an increase in Ω_{arag} with climate change. In these regions the surface ocean climate change response of pH and Ω_{arag} is dominated by ocean warming. The Arctic Ocean shows very different response to the other three regions. In the Arctic Ocean, DIC increases with climate change because of a reduction in sea-ice enables the ocean to come closer to equilibrium with the atmosphere. The increase in DIC with climate change provides a positive feedback for both Ω_{arag} and pH causing both variables to decrease with climate change..

5. Conclusion

Our study illustrates that pH and Ω_{arag} respond differently to climate change due to the ocean chemistry of CO_2. The dominating effects for the change in surface pH and Ω_{arag} with climate change are the direct (SST increases) and indirect (DIC reductions due to lower solubility) effects associated with warming. For pH, climate change feedbacks have little impact on the projected changes because the direct decrease in pH due to ocean warming is equal to but opposite in magnitude to the pH increase associated with lower DIC concentrations cause by a reduction in CO_2 solubility with ocean warming. This phenomenon is set-up by the carbonate chemistry and is therefore independent to the extent of ocean warming or the type of model used. Based on our analysis future oceanic acidification depends primarily on atmospheric CO_2 concentrations. The exception is in the high latitudes where changes in sea-ice extent elevate the degree of CO_2 saturation, which enhances the reduction of pH with climate change. For Ω_{arag}, our results show that climate change buffers the simulated decline by as much as 15%. As opposed to pH, the direct effect of ocean warming on Ω_{arag} is weak. The simulated climate change feedback on Ω_{arag} is therefore mainly controlled by DIC concentrations changes associated with solubility changes in CO_2 caused by ocean warming.

References

Anderson, L. G. and Jones, P. E. 1991. The transport of CO_2 into Arctic and Antarctic Seas : Similarities and differences in the driving processes. *J. Mar. Syst.* **2**, 81–95.

Barry, J. P., Buck, K. R., Lovera, C. F., Kuhnz, L., Whaling, P. J., Peltzer, E. T., and co-authors 2004. Effects of direct ocean CO_2 injection on deep-sea meiofauna. *J. Oceanogr.* **60**(4), 759–766.

Broecker, W. S. and Peng, T.-H. 1982. *Tracers in the Sea*. Eldigio Press, New York, 690 pp.

Caldeira, K. and Wickett, M. E. 2003. Anthropogenic carbon and ocean pH. *Nature* **425**(6956), 365–365.

Dickson, A. G. 1993. The measurement of sea water pH. *Mar. Chem.* **44**, 131–142.

Dickson, A. G. and Millero, F. J. 1987. A comparison of the equilibrium-constants for the dissociation of carbonic-acid in seawater media. *Deep-Sea Res. Part A—Oceanogr. Res. Papers* **34**(10), 1733–1743.

Engel, A., Zondervan, I., Aerts, K., Beaufort, L., Benthien, A., Chou, L., and co-authors 2005. Testing the direct effect of CO_2 concentration on a bloom of the coccolithophorid Emiliania huxleyi in mesocosm experiments. *Limnol. Oceanogr.* **50**(2), 493–507.

Gattuso, J. P., Frankignoulle, M., Bourge, I., Romaine, S. and Buddemeier, R. W., 1998. Effect of calcium carbonate saturation of seawater on coral calcification. *Global Planet. Change* **18**(1–2), 37–46.

Hirst, A. C., Gordon, H. B. and Ofarrell, S. P. 1996. Global warming in a coupled climate model including oceanic eddy-induced advection. *Geophys. Res. Lett.* **23**(23), 3361–3364.

Houghton, J. T., Ding, Y., Griggs, D. J., Noguer, M., Van der Linden, P. J. and Xiaosu, D. 2001. Climate Change 2001: The Scientific Basis. *Contribution of Working Group 1 to the Third Assessment Report of*

the Intergovernmental Panel on Climate Change (IPCC). Cambridge University Press, Cambridge, 944 pp.

Key, R. M., Kozyr, A., Sabine, C., Lee, K., Wanninkhof, R., Bullister, J. L., and co-authors 2004. A global ocean carbon climatology: Results from GLODAP. *Global Biogeochem. Cycles* **18**(4), GB4030.

Kikkawa, T., Ishimatsu, A. and Kita, J. 2003. Acute CO_2 tolerance during the early developmental stages of four marine teleosts. *Environ. Toxicol.* **18**(6), 375–382.

Kleypas, J. A., Buddemeier, R. W., Archer, D., Gattuso, J. P., Langdon, C. and Opdyke, B. N. 1999. Geochemical consequences of increased atmospheric carbon dioxide on coral reefs. *Science* **284**(5411), 118–120.

Langdon, C., Takahashi, T., Sweeney, C., Chipman, D., Goddard, J., Marubini, F., and co-authors 2000. Effect of calcium carbonate saturation state on the calcification rate of an experimental coral reef. *Global Biogeochem. Cycles* **14**(2), 639–654.

Matear, R. J. and Hirst, A. C. 1999. Climate change feedback on the future oceanic CO_2 uptake. *Tellus Ser. B-Chem. Phys. Meteorol.* **51**(3), 722–733.

McNeil, B. I., Matear, R. J. and Barnes, D. J. 2004. Coral reef calcification and climate change: The effect of ocean warming. *Geophys. Res. Lett.* **31**(22).

McNeil, B. I., Matear, R. J., Key, R. M., Bullister, J. L. and Sarmiento, J. L. 2003. Anthropogenic CO_2 uptake by the ocean based on the global chlorofluorocarbon data set. *Science* **299**(5604), 235–239.

McNeil, B. I., Tilbrook, B. and Matear, R. J. 2001. Accumulation and uptake of anthropogenic CO_2 in the Southern Ocean, south of Australia between 1968 and 1996. *J. Geophys. Res.-Oceans* **106**(C12), 31431–31445.

Orr, J. C., Fabry, V. J., Aumont, O., Bopp, L., Doney, S. C., Feely, R. A., and co-authors 2005. Anthropogenic ocean acidification over the twenty-first century and its impact on calcifying organisms. *Nature* **437**(7059), 681–686.

Pedersen, M. F. and Hansen, P. J. 2003a. Effects of high pH on a natural marine planktonic community. *Mar. Ecol.-Prog. Ser.* **260**, 19–31.

Pedersen, M. F. and Hansen, P. J. 2003b. Effects of high pH on the growth and survival of six marine heterotrophic protists. *Mar. Ecol.-Prog. Ser.* **260**, 33–41.

Portner, H. O., Langenbuch, M. and Reipschlager, A. 2004. Biological impact of elevated ocean CO_2 concentrations: Lessons from animal physiology and earth history. *J. Oceanogr.* **60**(4), 705–718.

Raven, J. 2005. Ocean acidification due to increasing atmospheric carbon dioxide. Document No. 12/05, The Royal Society, London.

Seibel, B. A. and Walsh, P. J. 2001. Carbon cycle - Potential, impacts of CO_2 injection on deep-sea biota. *Science* **294**(5541), 319–320.

Seibel, B. A. and Walsh, P. J. 2003. Biological impacts of deep-sea carbon dioxide injection inferred from indices of physiological performance. *J. Exp. Biol.* **206**(4), 641–650.

Sundquist, E. T., Plummer, L. N. and Wigley, T. M. L. 1979. Carbon dioxide in the ocean surface : The homogenous buffer factor. *Science* **204**(15 June), 1203–1205.

Walsh, P. J. and Milligan, C. L. 1989. Coordination of Metabolism and Intracellular Acid-Base Status - Ionic Regulation and Metabolic Consequences. *Can. J. Zool.-Revue Canadienne De Zoologie* **67**(12), 2994–3004.

Wanninkhof, R. 1992. Relationship Between Wind Speed and Gas Exchange Over the Ocean. *J. Geophys. Res.* **97**(C5), 7373–7382.

Watterson, I. G., Ofarrell, S. P. and Dix, M. R. 1997. Energy and water transport in climates simulated by a general circulation model that includes dynamic sea ice. *J. Geophys. Res.-Atmos.* **102**(D10), 11027–11037.